Eur Radiol (2017) 27:447–453
DOI 10.1007/s00330-016-4406-3

MUSCULOSKELETAL

Evaluation of chronic inflammatory demyelinating polyneuropathy: 3D nerve-sheath signal increased with inked rest-tissue rapid acquisition of relaxation enhancement imaging (3D SHINKEI)

Akio Hiwatashi[1] · Osamu Togao[1] · Koji Yamashita[1] · Kazufumi Kikuchi[1] · Hidenori Ogata[2] · Ryo Yamasaki[2] · Masami Yoneyama[3] · Jun-ichi Kira[2] · Hiroshi Honda[1]

Received: 29 September 2015 / Revised: 14 March 2016 / Accepted: 12 May 2016 / Published online: 21 May 2016

Abstract

Objective To evaluate the usefulness of 3D nerve-sheath signal increased with inked rest-tissue rapid acquisition of relaxation enhancement imaging (SHINKEI) in patients with chronic inflammatory demyelinating polyneuropathy (CIDP).

Methods This institutional review board-approved retrospective study included 14 CIDP patients and nine normal subjects. The signal-to-noise ratio (SNR), contrast ratio (CR), and the size of the cervical ganglions and roots were measured by two raters.

Results The SNRs of the ganglions and roots were larger in patients with CIDP (9.55 ± 3.87 and 9.81 ± 3.64) than in normal subjects (7.21 ± 2.42 and 5.70 ± 2.14, $P < 0.0001$, respectively). The CRs of the ganglions and roots were larger in patients with CIDP (0.77 ± 0.08 and 0.68 ± 0.12) than in normal subjects (0.72 ± 0.07 and 0.53 ± 0.11, $P < 0.0001$, respectively). The sizes of the ganglions and the roots were larger in patients with CIDP (6.44 ± 1.61 mm and 4.89 ± 1.94 mm) than in normal subjects (5.24 ± 1.02 mm and 3.39 ± 0.80 mm, $P < 0.0001$, respectively).

Conclusions Patients with CIDP could be distinguished from controls on 3D SHINKEI.

Key points

- *3D SHINKEI could visualize brachial plexus with high spatial resolution.*
- *CIDP patients showed increased SNR, CR, and the size of brachial plexus.*
- *3D SHINKEI could discriminate CIDP patients from normal subjects.*

Keywords Chronic inflammatory demyelinating polyneuropathy · Neurography · Brachial plexus · Magnetic resonance imaging · Demyelination

Abbreviations

3D SHINKEI	three-dimensional nerve-sheath signal increased with inked rest-tissue rapid acquisition of relaxation imaging
CIDP	chronic inflammatory demyelinating polyneuropathy
CR	contrast ratio
ICC	intraclass correlation coefficient
iMSDE	improved motion sensitized driven equilibrium
MR	magnetic resonance
ROC	receiver operating characteristics
ROI	region of interest
SD	standard deviation
SI	signal intensity
SNR	signal-to-noise ratio
SPAIR	spectral attenuated inversion recovery
STIR	short inversion time inversion-recovery

✉ Akio Hiwatashi
hiwatasi@radiol.med.kyushu-u.ac.jp

[1] Department of Clinical Radiology, Graduate School of Medical Sciences, Kyushu University, 3-1-1 Maidashi, Higashi-ku, Fukuoka 812-8582, Japan

[2] Departments of Neurology Graduate School of Medical Sciences, Kyushu University, Fukuoka, Japan

[3] MR Clinical Science, Philips Electronics Japan, Tokyo, Japan

Introduction

Chronic inflammatory demyelinating polyneuropathy (CIDP) is a demyelinating disease of the peripheral nerves, clinically heterogeneous, grossly symmetric, with sensory and motor neuropathy presenting as a monophasic, relapsing or progressive disorder [1–18]. It sometimes involves cervical nerves [4–7] and the brachial plexus [8]; however, these are relatively rare locations compared to the other peripheral nerves [5].

Magnetic resonance (MR) neurography [18–26] is a useful technique with which to evaluate abnormal conditions of entire nerves and nerve bundles [18–22]. It has been applied in patients with tumours, trauma, and neuritis of the brachial plexus [18, 20–22, 25]. Most commonly, a combination of fat-suppressed T2-weighted [with either frequency-selective or short inversion time inversion-recovery (STIR) sequences] and T1-weighted imaging sequences is used to evaluate diseases of the brachial plexus [18, 25]. In addition, Takahara et al developed MR neurography with diffusion-weighted imaging to visualize peripheral nerves [18].

Three-dimensional nerve-sheath signal increased with inked rest-tissue rapid acquisition of relaxation imaging (3D SHINKEI) is a new technique to suppress signals of blood vessels, muscles and fat tissue using improved motion-sensitized driven equilibrium (iMSDE) and spectral attenuated inversion recovery [23, 24]. With 3D SHINKEI, we can obtain images with high spatial resolution ($0.98 \times 0.97 \times 2.0$ mm^3) and quantitatively evaluate the cervical ganglions and roots of the brachial plexus. However, to the best of our knowledge, there has been no report using 3D SHINKEI to compare CIDP patients with normal subjects. Therefore, the purpose of this study was to evaluate the usefulness of 3D SHINKEI to distinguish patients with CIDP from normal subjects.

Materials and methods

This retrospective study was approved by our institutional review boards, and written informed consent was waived.

Patients

This study included 14 patients with CIDP (11 men and three women; age range 19-72 years old; median 45 years) who met the European Federation of Neurological Societies/Peripheral Nerve Society definite diagnostic criteria for CIDP from January 2012 to September 2014. The demographics of the patients are shown in Table 1. All patients underwent previous treatment with steroid (n = 8), intravenous immunoglobulin (n = 8), and vitamin B12 (n = 2). No patients showed immunoglobulinemia. In addition, nine normal subjects (five men and four women; age range 27-66 years old; median 45 years) were imaged.

Imaging technique

All patients underwent MR imaging with a 3.0-T system (Achieva TX, Philips, Best, the Netherlands) with a 16-

Table 1 Patients' demographics

No.	Age (years)	Sex	Previous Treatment	CSF protein	Dominant Extremities	Dominant Symptoms	Duration
1	19	M	Steroid	400	Lower	Motor = Sensory	3 years
2	27	M	Steroid	292	Upper = Lower	Sensory	8 months
3	29	M	Vit. B12	53	Upper = Lower	Sensory	1 years
4	38	M	Steroid	299	Upper	Motor	13 years
5	53	M	Steroid/IVIG	28	Upper	Motor	9 years
6	59	M	IVIG	103	Lower	Motor	8 years
7	59	M	Steroid/IVIG	50	Upper	Motor	3 years
8	62	M	Steroid/IVIG	30	Lower	Sensory	6 years
9	64	M	IVIG	59	Lower	Motor	6 years
10	68	M	Vit. B12	29	Upper	Sensory	9 years
11	72	M	IVIG	N/A	Lower	Motor	1 years
12	22	F	Steroid/IVIG	25	Upper	Motor	6 years
13	30	F	IVIG	59	Lower	Sensory	2 years
14	33	F	Steroid	74	Lower	Sensory	22 years

Note. Cerebrospinal fluid (CSF) was not obtained in one patient (#11) because of warfarin use

channel neurovascular coil. 3D SHINKEI, which was set as a research tool during the time of the study period, was obtained in the coronal plane as part of the cervical plexus MR neurography protocol. The details of 3D SHINKEI are described elsewhere [23, 24]. Briefly, it is a turbo spin echo with a diffusion-weighted prepulse called iMSDE and a spectral attenuated inversion recovery (SPAIR) fat suppression prepulse. The pre-pulse section of diffusion-prepared MR neurography consists of two parts; a fat-suppression pre-pulse and the iMSDE pre-pulse to suppress signals from vessels, followed by a readout section with a 3D tissue-specific variable refocusing flip-angle rapid acquisition with relaxation enhancement sequence to acquire contrast-efficient T2-weighting [23]. 3D SHINKEI parameters included TR/TE = 2400/74 ms, FOV = 220 × 310 mm, ETL = 100, matrix = 224 × 320, voxel size = 0.98 × 0.97 × 2.0 mm^3, b = 10 s/mm^2, iMSDE duration = 50 ms, phase encoding direction; right to left, percentage of phase oversampling; 50 %, acquisition time = 5 min 46 s.

Analysis

All MR images were transferred to picture archiving and communication systems (SYNAPSE; Fujifilm Medical, Tokyo, Japan). Regions of interest (ROIs) were placed at cervical ganglions and roots of the brachial plexus bilaterally at C5-T1 by neuroradiologists (A.H. and K.K., 18 and 10 years' experience in neuroradiology). The signal-to-noise ratio (SNR), the contrast ratio (CR), and the sizes of the ganglions and roots were measured. Circular- or linear-shaped ROIs were placed in the bilateral ganglions or roots at C5-T1 on coronal reformatted images of 3D SHINKEI [23]. The roots were measured adjacent to the ganglions in their largest diameters. Other circular-shaped ROIs were placed in the noise outside the body with the largest diameter possible. The SNR was calculated as follows: SNR = SI (ganglion or root)/SD (noise), where SI (ganglion or root) is the signal intensity of the ganglions or roots of brachial plexus, and SD (noise) is the standard deviation of the noise measured in the same ROI. The CR between the ganglion or root and the muscle (CR) was calculated as follows: CR = [SI (ganglion or root) - SI (muscle)]/[SI (ganglion or root) + SI (ganglion or root)], where SI (ganglion or root) is the signal intensity of the ganglions or roots, and SI (muscle) is the signal intensity of the muscles [23].

Statistical analyses were performed by one of the authors (A.H.) using JMP software (version 11.0.0; SAS Institute, Cary, NC, USA) and MedCalc Software (version 15.2; MedCalc, Mariakerke, Belgium) based on the measured locations (the ganglions and the roots of the brachial plexus from C5 to T1, bilaterally). Techniques used included the Mann-Whitney U test and receiver operating characteristics (ROC) curves. *P*-values less than 0.05 were considered significant. The Bonferroni correction was used for multiple comparisons. Interobserver agreement for each parameter from the two observers was analyzed by calculating the intraclass correlation coefficient (ICC), and Pearson correlation. ICCs are considered to be excellent when >0.74 [27]. Bland-Altman plot with the 95 % limits of agreement were also evaluated.

Results

The SNRs of the ganglions and roots were larger in patients with CIDP (mean ± SD; 9.55 ± 3.87 and 9.81 ± 3.64) than in normal subjects (7.21 ± 2.42 and 5.70 ± 2.14, $P < 0.0001$, respectively, Figs. 1, 2, and 3). The CRs of the ganglions and roots were larger in patients with CIDP (0.77 ± 0.08 and 0.68 ± 0.12) than in normal subjects (0.72 ± 0.07 and 0.53 ± 0.11, $P < 0.0001$, respectively). The sizes of the ganglions and the roots were larger in patients with CIDP (6.44 ± 1.61 mm and 4.89 ± 1.94 mm) than in normal subjects (5.24 ± 1.02 mm and 3.39 ± 0.80 mm, $P < 0.0001$, respectively). The sensitivity, specificity and the value of the area under the ROC curve were 0.507, 0.778, and 0.686 for the SNR (cutoff = 8.68), 0.364, 0.967 and 0.656 for the CR (cutoff = 0.81), and 0.479, 0.922 and 0.716 for the size (cutoff = 6.54) of the ganglions,

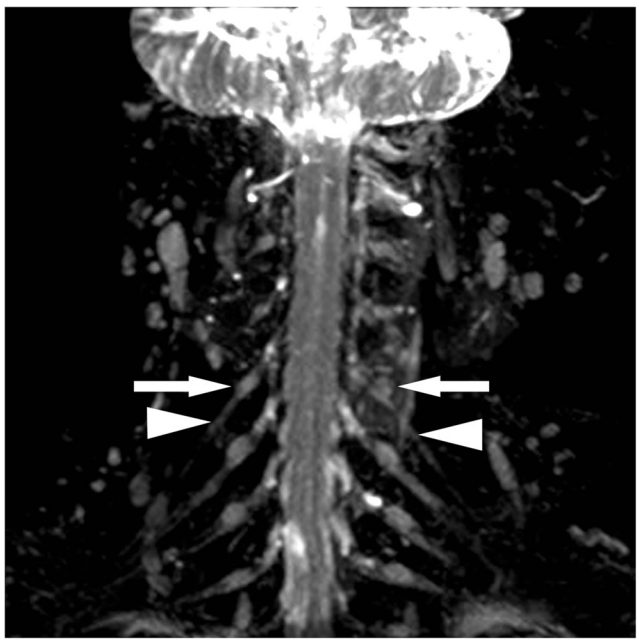

Fig. 1 A 54-year-old man of normal subject. The ganglions (*arrows*; C5) and the roots of the brachial plexus (*arrowheads*; C5) are well visualized

Fig. 2 A 39-year-old woman with CIDP. The ganglions (*arrows*; C5) and the roots of the brachial plexus (*arrowheads*; C5) are well visualized. These are swollen with increased signal compared to normal subject (Fig. 1)

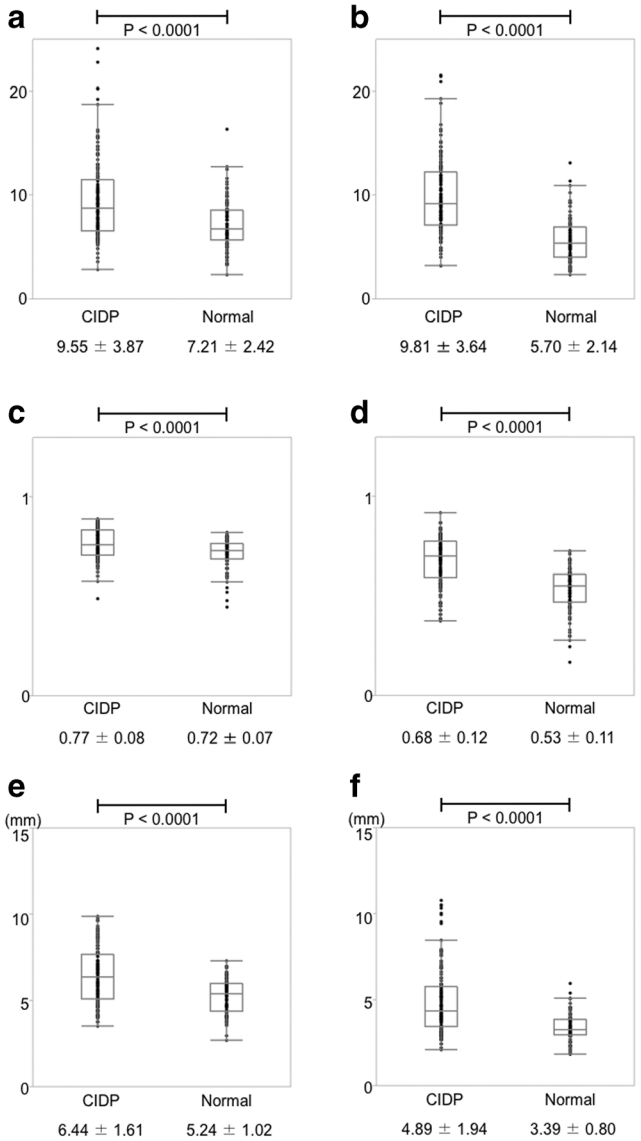

Fig. 3 SNR, CR, and size of the ganglions and roots. The SNRs of the ganglions (**a**) and roots (**b**) are larger in patients with CIDP (mean ± SD; 9.55 ± 3.87 and 9.81 ± 3.64) than in normal subjects (7.21 ± 2.42 and 5.70 ± 2.14, $P < 0.0001$, respectively). The CRs of the ganglions (**c**) and roots (**d**) are larger in patients with CIDP (0.77 ± 0.08 and 0.68 ± 0.12) than in normal subjects (0.72 ± 0.07 and 0.53 ± 0.11, $P < 0.0001$, respectively). The sizes of the ganglions (**e**) and the roots (**f**) are larger in patients with CIDP (6.44 ± 1.61 mm and 4.89 ± 1.94 mm) than in normal subjects (5.24 ± 1.02 mm and 3.39 ± 0.80 mm, $P < 0.0001$, respectively)

respectively (Fig. 4). These were 0.686, 0.878, and 0.850 for the SNR (cutoff = 7.81), 0.636, 0.911, and 0.813 for the CR (cutoff = 0.66), and 0.621, 0.822, and 0.757 for the size (cutoff = 3.99) of the roots, respectively. The area under the ROC curve was the largest for the SNR of the roots with statistically significant differences with the SNR, the CR, and the size of the ganglions ($P < 0.003$; Bonferroni correction). However, there were no statistically significant differences with the CR and the size of the roots ($P > 0.003$; Bonferroni correction).

Our evaluations of the interobserver agreement were 0.64 (95 % CI; 0.53 – 0.72) for the SNR, 0.76 (95 % CI; 0.68 – 0.81) for the CR, and 0.91 (95 % CI; 0.89 – 0.93) for the size of the ganglions ($P < 0.0001$, respectively; Fig. 5). These were 0.68 (95 % CI; 0.59 – 0.76) for the SNR, 0.75 (95 % CI; 0.68 – 0.81) for the CR, and 0.95 (95 % CI; 0.93 – 0.96) for the size of the roots ($P < 0.0001$, respectively).

Discussion

In this study we found that the SNR, CR, and diameter of the cervical ganglions and roots of the brachial plexus in patients with CIDP were larger than those in normal subjects on 3D SHINKEI. ROC analysis revealed that the SNR of the roots showed the best diagnostic performance. Because of the high spatial resolution ($0.98 \times 0.97 \times 2.0$ mm^3) and sufficient suppression of the signals of the fat, vessels, and muscles on 3D SHINKEI, this is the first report with a simultaneous quantitative evaluation of the signal intensity and size of the brachial plexus in patients with CIDP and normal subjects.

Previous qualitative studies have shown increased signal intensity on T2-weighted images in the brachial

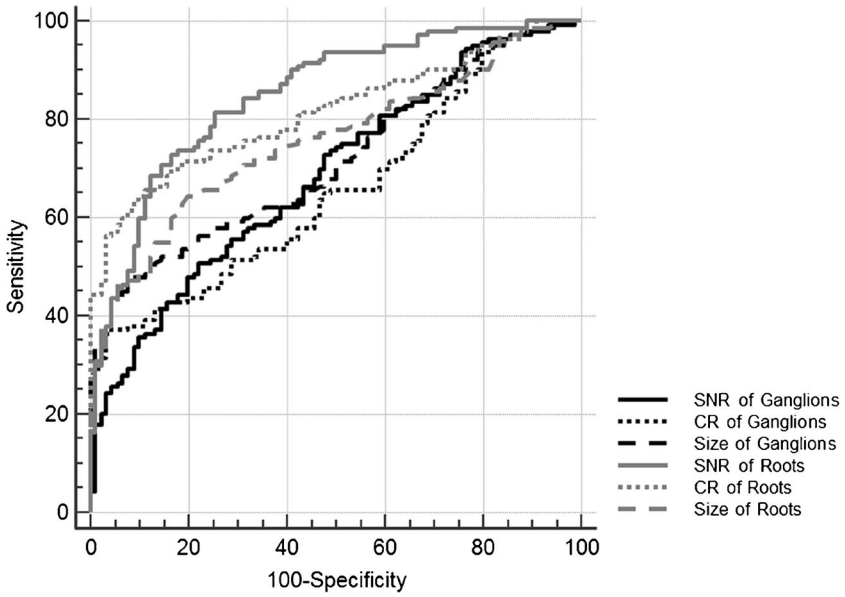

Fig. 4 The sensitivity, specificity and the value of the area under the ROC curve are 0.507, 0.778, and 0.686 for the SNR (cutoff = 8.68), 0.364, 0.967, and 0.656 for the CR (cutoff = 0.81), and 0.479, 0.922, and 0.716 for the size (cutoff = 6.54) of the ganglions, respectively. These are 0.686, 0.878, and 0.850 for the SNR (cutoff = 7.81), 0.636, 0.911, and 0.813 for the CR (cutoff = 0.66), and 0.621, 0.822, and 0.757 for the size (cutoff = 3.99) of the roots, respectively. The area under the ROC curve is the largest for the SNR of the roots with statistically significant differences with the SNR, the CR, and the size of the ganglions ($P < 0.003$; Bonferroni correction). However, there are no statistically significant differences with the CR and the size of the roots ($P > 0.003$; Bonferroni correction)

plexus or nerve trunks in patients with CIDP [3, 8–13]. Historically, Symonds et al reported finding nerve root enlargement on myelography of CIDP patients [14]. Matsuoka et al also reported the enlarged cervical nerve roots on ultrasound [3]. Midoroni et al also reported that the nerve roots were enlarged, most significantly in the extraforaminal region [15]. Qualitative assessment of the nerve hypertrophy also has been reported on MR [13]. These are likely representing recurrent demyelination and remyelination pathologically. Recently, Tanaka et al used STIR for quantitative evaluation of the cervical nerves in patients with CIDP on a 1.5 T-scanner. They showed the increased contrast-to-noise ratios at the C5, C6, C7, and C8 nerve roots, but failed to show increased sizes in these roots. We believe that the adequate suppression of the background signal and high spatial resolution with our technique could verify the difference of the size simultaneously.

Our evaluations of the interobserver agreement were excellent for the CR and the size of the ganglions and the roots; however, these were not for the SNR. Because the SNR was calculated by SI divided by the SD, the variations tended to be larger than the CR and the size. The ICC for the SNR in this study were 0.64 in the ganglions and 0.68 in the roots, which might be acceptable.

Contrast enhancement in the peripheral nerves is also known in inflammatory and demyelinating diseases [3, 8, 12, 15, 16, 28]. Midroni et al have reported seeing contrast enhancement of the cauda equina in 69 % of their CIDP patients and none of their control subjects [15]. Several studies have revealed abnormal enhancement of spinal nerve roots [8, 12, 16], which has also been demonstrated in Guillain–Barré syndrome [28]. Hypertrophy of nerve roots has often been described in combination with abnormal enhancement [3, 8, 16], showing spinal stenosis in some cases [3, 16]. Another study with diffusion-weighted imaging has also been reported. Tanaka et al reported that the diffusivity in the plexuses of patients and normal volunteers were $1.27 \pm 0.43 \times 10^{-3}$ mm^2/s and $0.92 \pm 0.11 \times 10^{-3}$ mm^2/s, respectively [17]. We have not used contrast-enhanced and diffusion-weighted imaging. We need further evaluation of the clinical utility of these techniques and current results.

There are several limitations to this study. We did not evaluate the distal portion of the brachial plexus. Because of its complex form, we think it is extremely difficult to evaluate the entire length of the plexus. We sometimes experience insufficient fat suppression. Use of DIXON, not SPAIR in 3D SHINKEI, is suitable to evaluate the entire brachial plexus. We are developing the "improved" 3D SHINKEI with DIXON. There are difficulties in calculating the SNR in parallel imaging [29]; therefore, we used SD of the same ROI in the ganglions or the roots, not in the air. Lack of contrast material is another limitation in this study. Because the

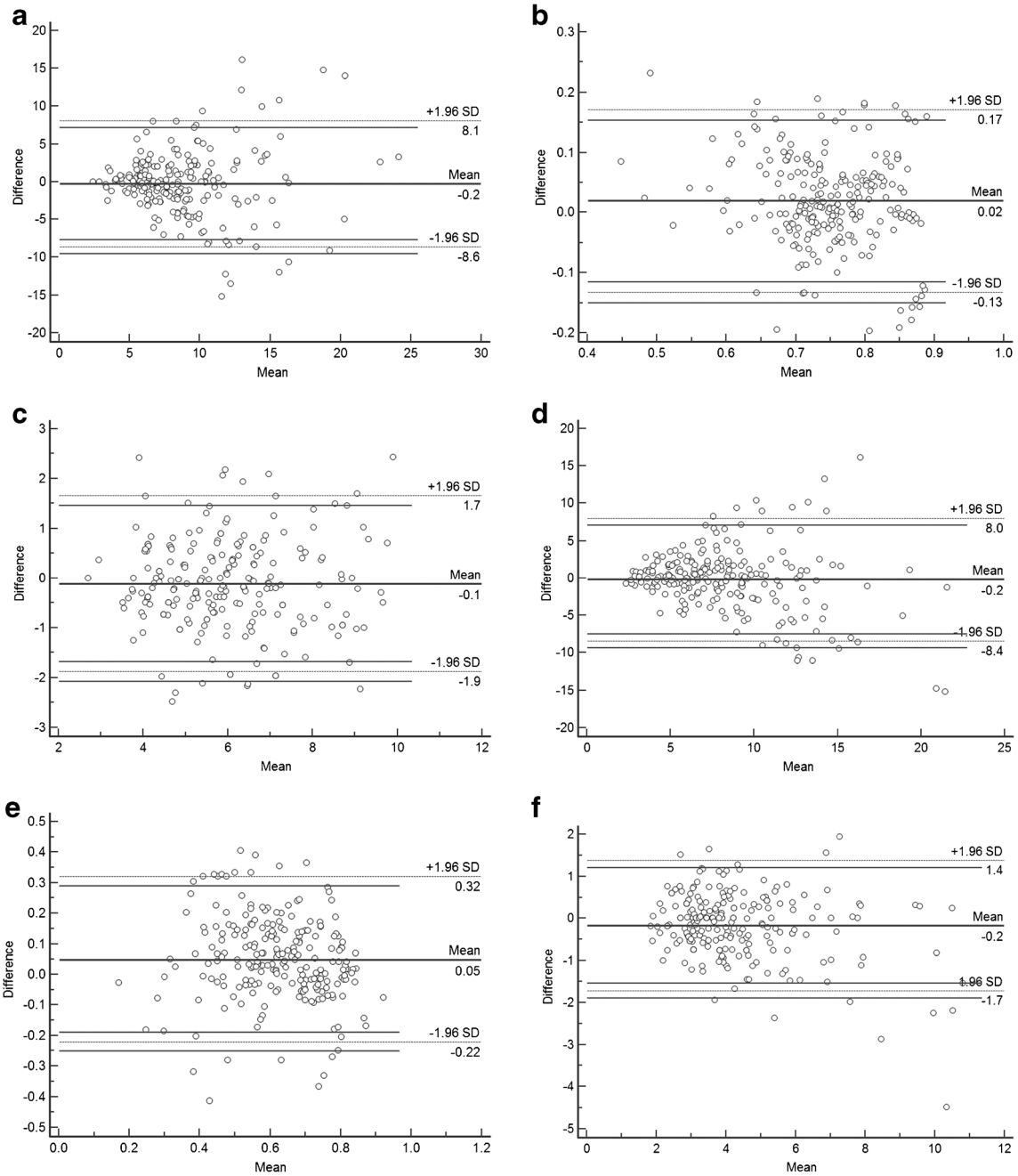

Fig. 5 Bland-Altman plot and 95 % limits of agreement. Our evaluations of the interobserver agreement are 0.64 (95 % CI; 0.53 – 0.72) for the SNR (**a**), 0.76 (95 % CI; 0.68 – 0.81) for the CR (**b**), and 0.91 (95 % CI; 0.89 – 0.93) for the size (**c**) of the ganglions, respectively. These are 0.68 (95 % CI; 0.59 – 0.76) for the SNR (**d**), 0.75 (95 % CI; 0.68 – 0.81) for the CR (**e**), and 0.95 (95 % CI; 0.93 – 0.96) for the size (**e**) of the roots, respectively

symptoms of almost all patients were stable, most of the patients refused to use the contrast. The small number of patients included and lack of the evaluation of the other nerves might be other limitations. We are continuing to gather patient data with more sophisticated techniques. ROC analysis revealed that the SNR of the roots showed the best diagnostic performance; however, it might be difficult to apply in our clinical practice because of the overlaps between two groups.

In conclusion, with 3D SHINKEI we obtained high-resolution MR neurography in cervical ganglions and roots. Patients with CIDP were distinguished from normal subjects on 3D SHINKEI.

Acknowledgments The scientific guarantor of this publication is Hiroshi Honda. The authors of this manuscript declare relationships with the following companies: Philips Electronics Japan. The authors state that

this work was supported by JSPS KAKENHI Grant Number 26461826. Mr. Junji Kishimoto kindly provided statistical advice for this manuscript. Institutional Review Board approval was obtained. Written informed consent was waived by the Institutional Review Board. Some study subjects or cohorts have been previously reported at ASNR 2015. Methodology: retrospective, observational, performed at one institution.

References

1. Joint Task Force of the EFNS and the PNS (2010) European federation of neurological societies/peripheral nerve society guideline on management of paraproteinemic demyelinating neuropathies. Report of a joint task force of the European federation of neurological societies and the peripheral nerve society–first revision. J Peripher Nerv Syst 15:185–195
2. Tanaka K, Mori N, Yokota Y, Suenaga T (2013) MRI of the cervical nerve roots in the diagnosis of chronic inflammatory demyelinating polyradiculoneuropathy: a single-institution, retrospective case-control study. BMJ Open 3:e003443
3. Matsuoka N, Kohriyama T, Ochi K et al (2004) Detection of cervical nerve root hypertrophy by ultrasonography in chronic inflammatory demyelinating polyradiculoneuropathy. J Neurol Sci 219:15–21
4. Dyck PJ, Lais AC, Ohta M, Bastron JA, Okazaki H, Groover RV (1975) Chronic inflammatory polyradiculoneuropathy. Mayo Clin Proc 50:621–637
5. Bradley LJ, Wilhelm T, King RH, Ginsberg L, Orrell RW (2006) Brachial plexus hypertrophy in chronic inflammatory demyelinating polyradiculoneuropathy. Neuromuscul Disord 16:126–131
6. Duarte J, Martinez AC, Rodriguez F, Mendoza A, Sempere AP, Claveria LE (1999) Hypertrophy of multiple cranial nerves and spinal roots in chronic inflammatory demyelinating neuropathy. J Neurol Neurosurg Psychiatry 67:685–687
7. Midroni G, Dyck PJ (1996) Chronic inflammatory demyelinating polyradiculoneuropathy: unusual clinical features and therapeutic responses. Neurology 46:1206–1212
8. Duggins AJ, McLeod JG, Pollard JD et al (1999) Spinal root and plexus hypertrophy in chronic inflammatory demyelinating polyneuropathy. Brain 122:1383–1390
9. Mizuno K, Nagamatsu M, Hattori N et al (1998) Chronic inflammatory demyelinating polyradiculoneuropathy with diffuse and massive peripheral nerve hypertrophy: distinctive clinical and magnetic resonance imaging features. Muscle Nerve 21:805–808
10. Kuwabara S, Nakajima M, Matsuda S, Hattori T (1997) Magnetic resonance imaging at the demyelinative foci in chronic inflammatory demyelinating polyneuropathy. Neurology 48:874–877
11. Van Es HW, Van den Berg LH, Franssen H et al (1997) Magnetic resonance imaging of the brachial plexus in patients with multifocal motor neuropathy. Neurology 48:1218–1224
12. De Silva RN, Willison HJ, Doyle D, Weir AI, Hadley DM, Thomas AM (1994) Nerve root hypertrophy in chronic inflammatory demyelinating polyneuropathy. Muscle Nerve 17:168–17170
13. Tazawa K, Matsuda M, Yoshida T et al (2008) Spinal nerve root hypertrophy on MRI: clinical significance in the diagnosis of chronic inflammatory demyelinating polyradiculoneuropathy. Intern Med 47:2019–2024
14. Symonds CP, Blackwood W (1962) Spinal cord compression in hypertrophic neuritis. Brain 85:251–260
15. Midroni G, de Tilly LN, Gray B, Vajsar J (1999) MRI of the cauda equina in CIDP: clinical correlations. J Neurol Sci 170:36–44
16. Kitakule MM, McNeal A (1997) Massive nerve root hypertrophy in chronic inflammatory demyelinating polyradiculoneuropathy. J Assoc Acad Minor Phys 8:55–57
17. Adachi Y, Sato N, Okamoto T et al (2011) Brachial and lumbar plexuses in chronic inflammatory demyelinating polyradiculoneuropathy: MRI assessment including apparent diffusion coefficient. Neuroradiology 53:3–11
18. Takahara T, Hendrikse J, Yamashita T et al (2008) Diffusion-weighted MR neurography of the brachial plexus: feasibility study. Radiology 249:653–660
19. Filler AG, Howe FA, Hayes CE et al (1993) Magnetic resonance neurography. Lancet 341:659–661
20. Filler AG, Kliot M, Howe FA et al (1996) Application of magnetic resonance neurography in the evaluation of patients with peripheral nerve pathology. J Neurosurg 85:299–309
21. Filler AG, Haynes J, Jordan SE et al (2005) Sciatica of nondisc origin and piriformis syndrome: diagnosis by magnetic resonance neurography and interventional magnetic resonance imaging with outcome study of resulting treatment. J Neurosurg Spine 2:99–115
22. Hayes CE, Tsuruda JS, Mathis CM, Maravilla KR, Kliot M, Filler AG (1997) Brachial plexus: MR imaging with a dedicated phased array of surface coils. Radiology 203:286–289
23. Yoneyama M, Takahara T, Kwee TC, Nakamura M, Tabuchi T (2013) Rapid high resolution MR neurography with a diffusion-weighted pre-pulse. Magn Reson Med Sci 12:111–119
24. Kasper JM, Wadhwa V, Scott KM, Rozen S, Xi Y, Chhabra A (2015) SHINKEI-a novel 3D isotropic MR neurography technique: technical advantages over 3DIRTSE-based imaging. Eur Radiol 25: 1672–1677
25. Yoshida T, Sueyoshi T, Suwazono S, Suehara M (2015) Three-tesla magnetic resonance neurography of the brachial plexus in cervical radiculopathy. Muscle Nerve 52:392–396
26. Chhabra A, Belzberg AJ, Rosson GD et al. (2015) Impact of high resolution 3 tesla MR neurography (MRN) on diagnostic thinking and therapeutic patient management. Eur Radiol
27. Shrout PE (1979) Fleiss JL (1979) Intraclass correlations: uses in assessing rater reliability. Psychol Bull 86:420–428
28. Gorson KC, Ropper AH, Muriello MA, Blair R (1996) Prospective evaluation of MRI lumbosacral nerve root enhancement in acute Guillain-Barré syndrome. Neurology 47:813–817
29. Dietrich O, Raya JG, Reeder SB, Reiser MF, Schoenberg SO (2007) Measurement of signal-to-noise ratios in MR images: influence of multichannel coils, parallel imaging, and reconstruction filters. J Magn Reson Imaging 26:375–385